

# Structural Health Monitoring of Wind Turbine Blade

Subjects: [Materials Science](#), [Composites](#)

Contributor: Mickaël Castro , Jean-Francois FELLER , Antoine Lemartinel , , Julio De-Luca

The growing demands for electrical energy, especially renewable, is boosting the development of wind turbines equipped with longer composite blades. To reduce the maintenance cost of huge composite parts, the structural health monitoring (SHM) is an approach to anticipate and/or follow the structural behaviour along time. Apart from the development of traditional non-destructive testing methods, in order to reduce the use of intrusive instrumentation there is a growing interest for the development of “self-sensing materials”. An interesting route to achieve this, can be to introduce carbon nanofillers such as nanotubes (CNT) in the composite structures, which enables to create systems that are sensitive to both strain and damage.

composite materials

structural health monitoring (SHM)

fibre-reinforced plastics (FRP)

nano engineered composites

carbon nanotubes (CNT)

## 1. Introduction

Structural Health Monitoring (SHM) system, which would provide clues about the material's health state, comes out as a very interesting tool [\[1\]\[2\]\[3\]\[4\]](#). SHM systems have multiple objectives, such as allowing an optimal use of the structure, decreasing the downtime, and avoiding catastrophic failure. It should also help to replace the scheduled and periodic maintenances by performance-based inspections; as well as to reduce the human involvement for less labour, human errors, and therefore higher reliability. Structural Health Monitoring (SHM) of wind turbine blades is required, because their failure is one of the main reasons for turbine downtimes [\[5\]](#). Today's main causes of damages in blades are identified as follows [\[6\]](#): Firstly, the erosion of the leading edge, mainly close to the tip, caused by abrasive airborne particles, and reduces the aerodynamic efficiency. It can also create delamination along the edge. Secondly, the lightning can induce damages and cracks around the impact point. Then, the accumulation of ice on the blade's surface, due to the combination of climate and temperature conditions, can result in a reduction of the aerodynamic or an increase of the fatigue caused by the additional mass.

Wind turbines have an expected life time of 20 years. The degradation of blades due to fatigue mechanisms is therefore likely to happen before the end of life and requiring reparations after a pertinent diagnosis. The resulting damages proposed by Sørensen et al. [\[7\]](#) are shown in **Figure 1**.

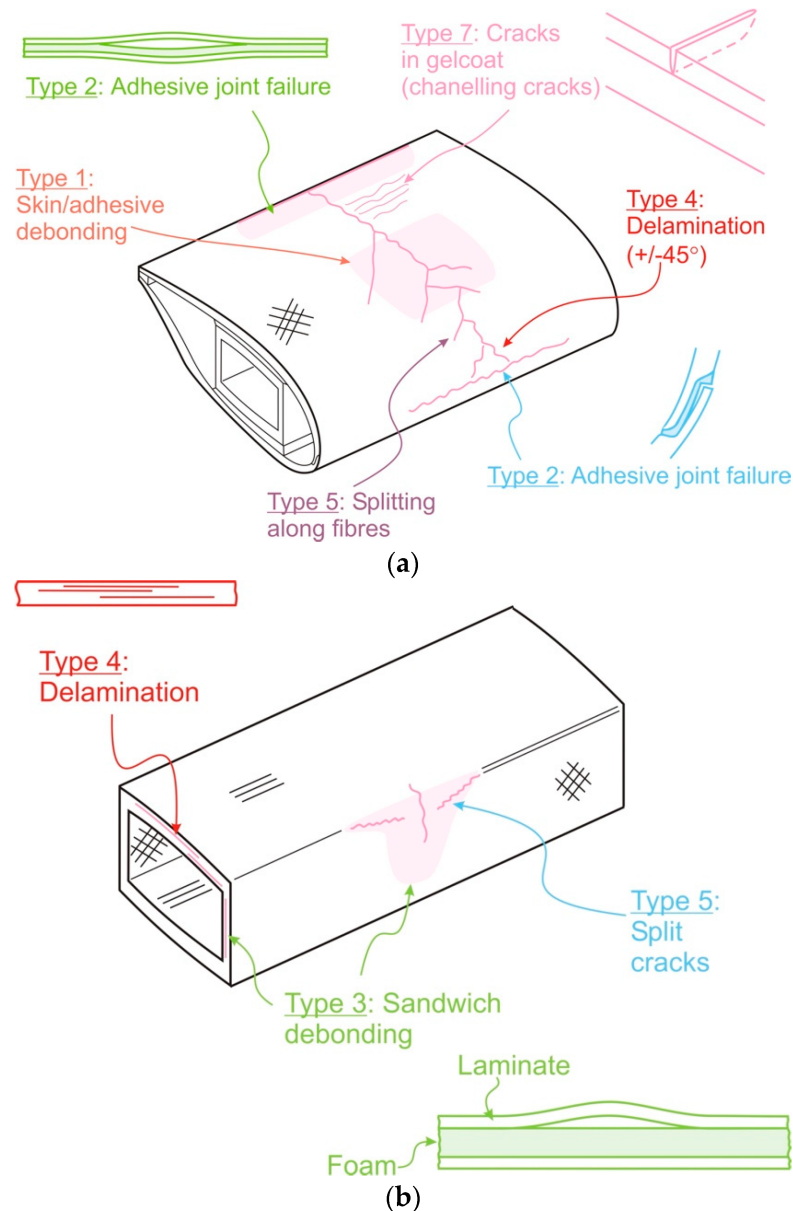


**Figure 1.** Sketches of the different types of damage that can occur in a wind turbine blade, (a) by skin-adhesive debonding, (b) delamination [7].

The different sketches of damage can be classified in 7 types:

- Type 1: Damage formation and growth in the adhesive layer joining skin and main spar flanges (skin/adhesive debonding and/or main spar/adhesive layer debonding),
- Type 2: Damage formation and growth in the adhesive layer joining the up and downwind skins along leading and/or trailing edges (adhesive joint failure between skins),
- Type 3: Damage formation and growth at the interface between face and core in sandwich panels in skins and main spar web (sandwich panel face/core debonding),

- Type 4: Internal damage formation and growth in laminates in skin and/or main spar flanges, under a tensile or compression load (delamination driven by a tensional or a buckling load),
- Type 5: Splitting and fracture of separate fibres in laminates of the skin and main spar (fibre failure in tension; laminate failure in compression),
- Type 6: Buckling of the skin due to damage formation and growth in the bond between skin and main spar under compressive load (skin/adhesive debonding induced by buckling, a specific type 1 case),
- Type 7: Formation and growth of cracks in the gel-coat; debonding of the gelcoat from the skin (gel-coat cracking and gel-coat/skin debonding).

Furthermore, off-shore wind turbines are exposed to harsh environmental conditions (humidity, salinity, varying temperature...) and fluctuating load that affect the system's performance and ultimately provoke a failure. A fault is defined as a significant change in the system parameters beyond *acceptable/allowed* limits leading to a decrease of the system performance. Depending on the fault and the related criticality, the required actions may include corrective maintenance intending to restore the system to its previous (undamaged) state or emergency maintenance targeting to avoid failures of components and systems. To avoid the downtime of the structure, as well as localising failures and predicting the remaining life time of blades, the development of SHM techniques is inevitable, keeping in mind, at the same time, its beneficial impact on the operating and maintenance costs. In a laminate composite material, damage initiates and propagates in zones of high-stress concentrations, such as free edges around cut-outs, joints or delamination edges [\[6\]](#)[\[8\]](#)[\[9\]](#).

## 2. Commercially Available Technics Based on Strain & Damage Monitoring

The basic principle of strain gauges is to provide the variation of length of the material on defined zones. The damage undergone by a structure is not directly obtained by the strain gauges. Using the resistance laws of materials (Hooke's laws), the stress can be calculated from the deformation, where the sensor is located [\[1\]](#). The knowledge of the mechanical properties of the material is therefore necessary to use strain gauges. Different types of gauges can be found but their principle is similar: any strain undergone by the gauge is directly converted into an electrical or optical signal as an output. Once a gauge is attached to the structure, its deformation is locally similar to the one encountered by the structure. Thus, the gauge signal recording enables an estimation the structure's deformation. The existing strain gauges mainly rely on capacitance, inductance or resistance of the sensing element, and on transmitted or reflected signals of optical fibres [\[1\]](#)[\[10\]](#)[\[11\]](#)[\[12\]](#).

### 2.1. Monitoring Technics Used in Strain Analysis

#### 2.1.1. Metallic Strain Gauges

The elastic deformation of a metal gauge proportionally modifies the value of its resistance. The sensitivity, or gauge factor (GF), of strain gauges is generally in the order of 2 and the initial resistances can vary from 30  $\Omega$  to 3 k $\Omega$ . The value of the initial resistance, as well as the gauge factor, is precisely set and controlled. The non-linear characteristic of metal gauge usually starts with strains up to  $\pm 15\%$  [13]. For smaller deformation, there is an emergence of new strain gauges with much higher gauge factors, up to 150 [14]. In general, these sensors are preferably positioned on the surface of the structure, possess limited sensitivity towards direction over a defined area [15], and have a flat surface allowing an optimised adhesion. Since the patent of the printed circuit for foil strain gauge in 1952 by Paul Eisler [16] the technic has obviously become mature. It is a precise and affordable technology with a standard deviation of the GF value about 1% [13], and a price around 10 € per direction of measurement [17].

### 2.1.2. Optical Fibres

Several technologies based on optical fibres (OF) already exist, with a predominance of fibre Bragg grating (FBG) or Rayleigh scattering [18]. A FBG sensor is a periodic variation of the refractive index in the fibre's core (**Figure 2**). The change of the core refraction index is between  $10^{-5}$  and  $10^{-3}$ , and the length of a Bragg grating is usually around 10 mm [19]. When an emitted light along the fibre arrives on the sensor, the change of the refraction index induces the creation of a transmitted and a reflected light signal as shown in **Figure 2**.

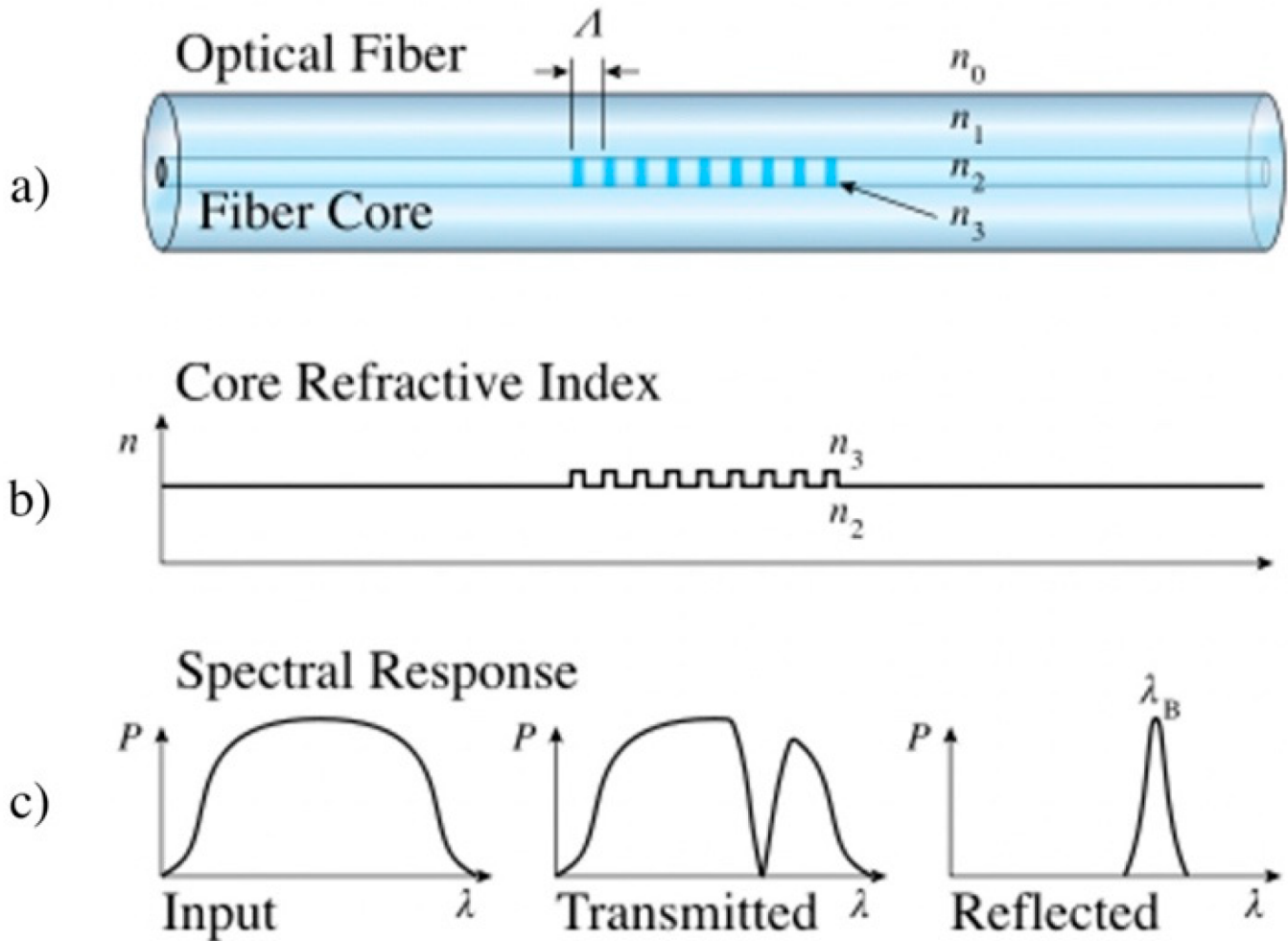


**Figure 2.** Principle of a FBG sensor [20]. (a) A Fibre Bragg Grating structure with the different refractive index (outer  $n_0$ , fibre  $n_1$ , core  $n_2$ , and grating  $n_3$ ) and the distance  $\Lambda$  between each grating. (b) The refractive core index profile. (c) Illustration of the transmitted and reflected spectral response regarding the input signal.

Any change of the refraction index in the grating modifies the transmitted and reflected signal. External solicitation such as strain, temperature, humidity, vibrations, breaks and delamination can induce a change in the index [10][19][20][21][22][23][24][25].

Therefore, any local strain or temperature modification can be measured by FBG sensors. Several FBG sensors can be grated along a single OF. A discrete mapping of a structure can therefore be assumed by a unique fibre. In order to discriminate between the strain and the temperature via the wavelength shift, the use of two different optical fibres is requested in practice [26].

Rayleigh scattering optical fibres have a refractive index which varies along the fibre as a function of the presence of defects or non-homogeneities of the material [11]. This index variation allows backscattering of different wavelengths at different points of the fibre. The analysis of the backscattered light makes possible to obtain information on the deformation, the changes in temperature, and the undergone flexion at each point along the

fibre. Compared to FBG, the strain deformation can be estimated along the complete fibre, thus inducing a larger amount of data.

FBG or Rayleigh fibres can be surface-applied or integrated in the structure. On the surface, they do not modify the characteristics of the material. Once in the core of the composite, the optical fibre size, usually about 100–150  $\mu\text{m}$ , is much greater than the composites reinforcing fibres, less than 20  $\mu\text{m}$  for carbon or glass fibres. It results in the creation of a gap between the optical fibres and the reinforcement fibres, as shown in **Figure 3**, thus inducing resin rich regions.

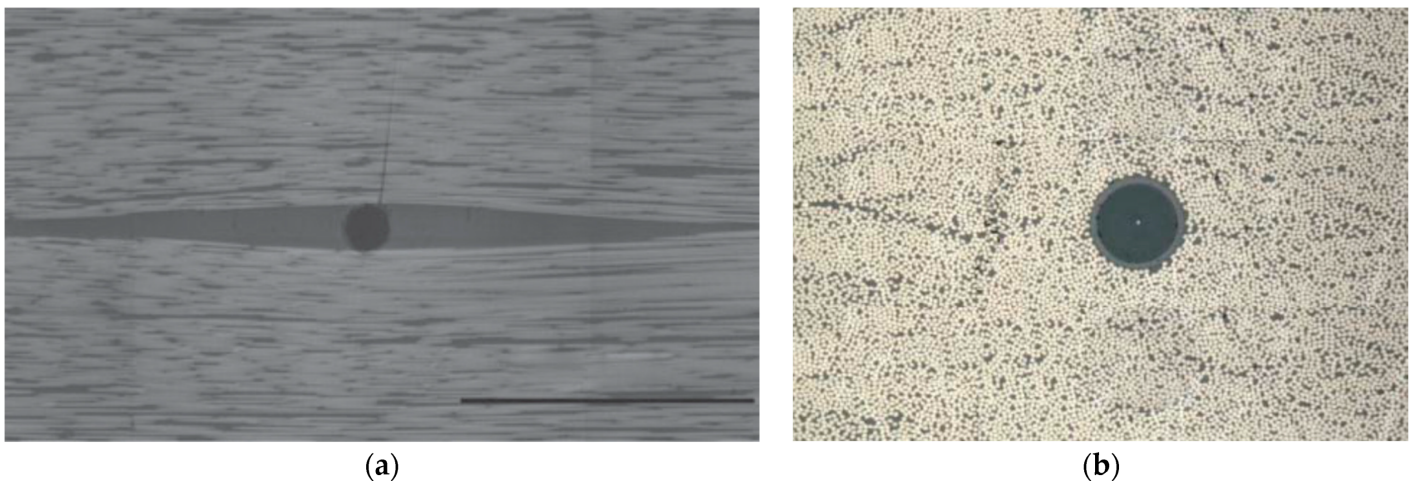


**Figure 3.** OF embedded in a composite (a) perpendicularly to the fibres (diameter 80  $\mu\text{m}$  and scale bar 500  $\mu\text{m}$ ) [27] and (b) in the fibres axis (diameter 125  $\mu\text{m}$ ) [28].

## 2.2. Monitoring Techniques Used in Failure Analysis

### 2.2.1. Visual Inspection

To date, the periodic structural health inspection of wind turbine blades is made by professional climbers while the wind turbine is shut down. The inspection is mainly limited to visual inspection and simple manual tapping tests with a hammer [29][30]. It allows detecting surface damages in defined critical areas. For internal damages, the tapping method requires an expertise to distinguish between the damaged and undamaged structure.

### 2.2.2. Performance Analysis

A wind turbine structure, working in its optimal state, exhibits a certain level of performance (power, nominal voltage, angle of inclination of the blades, current, speed of the blades, etc.). When the structure degrades, performance is changed despite identical operating conditions [31]. Consequently, the analysis of various operating parameters enables to identify the presence of damages on the structure when deviations are important compared to the optimum performances [10][12].

### 2.2.3. Acoustic Emission (AE)

Acoustic Emission (AE) is known as the emission of elastic waves with low amplitude ranges and high frequency (from 100 kHz to 1 MHz) [1][32]. The AE waves are generated within the material by the release of energy. Therefore, AE is a passive non-destructive evaluation technic (NDE) because the excitation source is the core material without any additional external source. Typical sources of AE are initiation and propagation of cracks, breakage of fibres, fracture of the matrix, friction between different surfaces, deformation, delamination, and impacts [1][33]. The detection of the AE waves is made by a surface sensor. The different failures in the structure can be detected depending on different characteristics of the emitted signal, i.e., counts, rise time, peak amplitude, arrival time, duration, and signal energy content [32]. This technique is commonly used in the industry for the control of composites [30][34][35], and allows steady-state wind turbine blade control [1]. This method is already protected with several patents [36][37][38][39].

#### 2.2.4. Ultrasonic Measurements

Unlike acoustic emission, which is a passive NDE, ultrasonic measurement (US) is an active monitoring technic. In addition to the received signal, an external excitation source is emitted. This signal propagates within the structure, is thus affected by the material which modified its characteristics (change of phase, defect, delamination, interfacial problems...) [33][10][35][40]. The use of ultrasonic waves enables to obtain information on the material's state. Three main techniques exist, named *pulse-echo*, *thickness*, and *pitch-catch* as illustrated in **Figure 4**. In *echo-pulse* mode, the wave is sent orthogonally to the material by a transducer which is attached to the surface. The reflection of the wave allows to obtain information on the various defects (type, depth). In *thickness* mode, the wave is sent through the thickness of the structure, and the reflected wave enables to collect similar information as that in the *pulse-echo* mode.

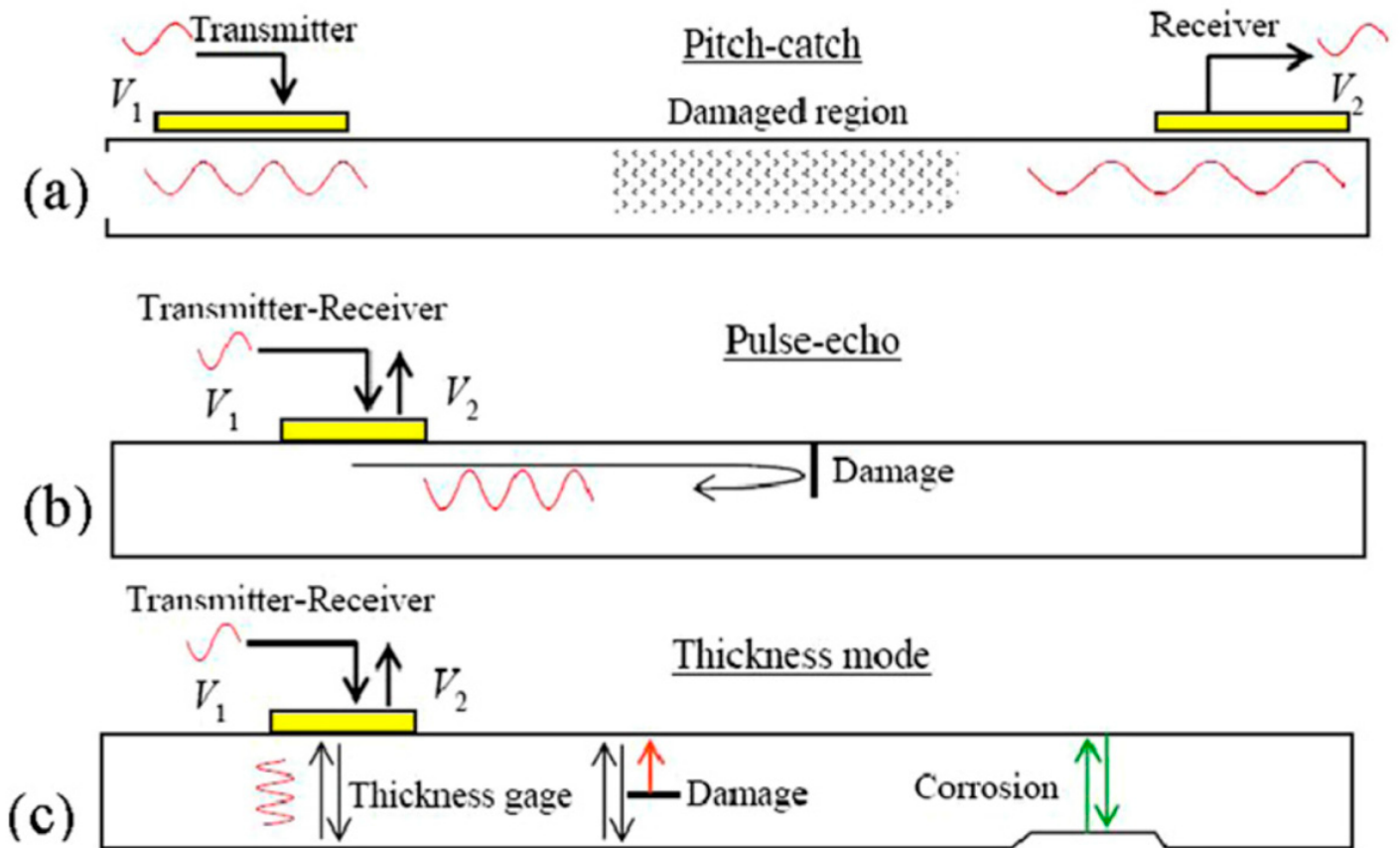


**Figure 4.** Damage detection with propagating and standing guided waves: (a) pitch-catch, (b) pulse-echo, and (c) thickness mode [41].

### 2.2.5. Vibrational Analysis

The analysis of a structure vibrations parameters, such as the frequency, and their variation, enables to measure the structure deformation and the appearance and propagation of cracks [10][40]. Depending on the vibration frequencies, varying from 0.01 Hz to 100 kHz [40], different sensors are used, from motion and speed sensors to accelerometers and emitted energy sensor. This technic has been identified as promising and patented in the field of wind blades [42].

### 2.2.6. Radiography

Observation by X-ray in transmission provides an image of the state of the material [31]. **Figure 5a**, produced by Tan et al. [43], shows an X-ray images of a 6.1 mm thick CFRP laminate after a 6.7 J impact, where different resulting damages have been identified. As shown in **Figure 5b** with a 3D reconstruction of a GFRP sample, this technique enables to identify the presence of defects such as breaks, delaminations, lacks of adhesive, vacuums, or shifts in the fibres orientation [33][10][40][44]. The detection limit is about 10  $\mu\text{m}$ , and this technique is sensitive to a variation of up to 1–2% of the material thickness. It is also possible to retrieve information on the variation of the materials' density from the backscattering of X-rays. This technique enables to quickly obtain a state of the structure because the set of images is obtained simultaneously. On the other hand, it is a complicated technique to

implement because it requires greater security measures due to the X-rays hazard. It is therefore used to control the quality of the structure after manufacturing.

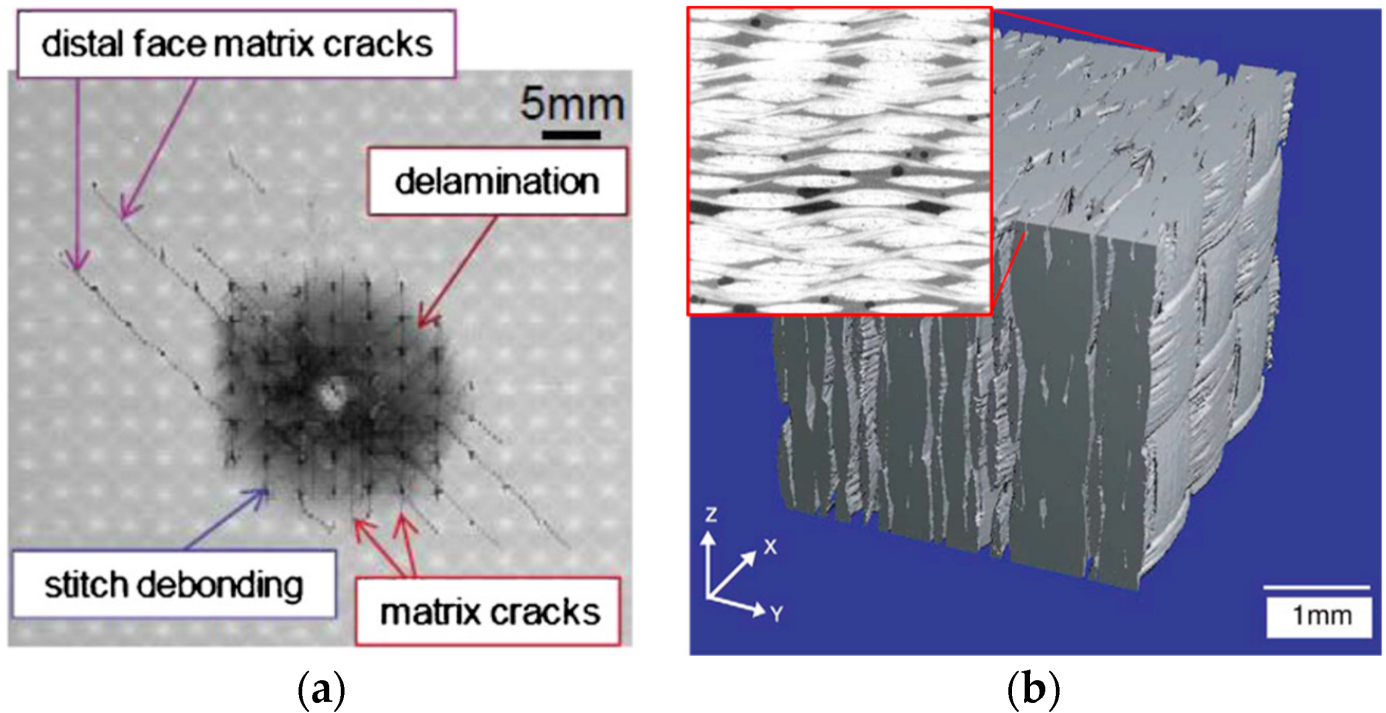


**Figure 5.** (a) X-ray radiography of a 6.1 mm thick CFRP laminate after a 6.7 J impact [43]. (b) 3D-reconstruction of a part of a GFRP sample by radiography. Insert shows a slice of the reconstruction where voids can be seen in black [44].

### 2.2.7. Optical Fibres (OF)

Optical fibres (OF) were originally used as a strain sensor for structures. The first appearance of OF to detect damages in composites was introduced by Hofer in 1987 [45].

## 3. Emerging Technics Based on Self-Sensing Thermoset Composites Filled with Carbon Materials

The classical SHM and maintenance technics previously described have shown to be efficient methods for strain and damage detection. Nevertheless, most of them require either an extensive human involvement or expensive procedures. Moreover, they present partial information of the structure since they are only sensitive to strain or damage. Consequently, the combination of complementary technics appears compulsory for a suitable SHM system. To date, the use of optical fibres is the most promising technique, because firstly it can provide, at a laboratory scale, both strain and specific damages, and, secondly, unlike the other technics, the optical fibres could be embedded in the core of composite structures (their detrimental effects on the mechanical properties being acceptable). Nevertheless, their sensitivity remains lower than that of commercial metallic strain gauges, and a substantial equipment is required, as well for the fibres' deployment as for the *in-service* use. Consequently, in

parallel with the previously mentioned strategies, there has been a growing interest for the development of “self-sensing materials”. Those materials are prone to provide real-time information about themselves or their environment [2].

### 3.1. Carbon Fibre Reinforced Epoxy (CF-EP) as Self-Sensing Materials

In 1989, Schulte and Baron [46], while studying carbon fibres reinforced epoxy, were the first to report the direct use of carbon fibres' resistance change as piezo-resistive sensing strategy. As observed in **Figure 6a**, the change of resistance was linear with the strain until the first fibre fracture at 0.7%, followed by a larger change of resistance and finally infinite resistance at the breakage of the sample. They reported an initial resistivity of 332  $\Omega\cdot\text{m}$  (2.5 M $\Omega$  for a 19 cm long sample), and a 0.6% change of resistance at 1.0% of deformation. Similar results have been reported by Wang et al. [47] with a sample of epoxy reinforced with 5.5 vol.% of short carbon fibres, and Todoroki et al. [48][49] mentioned that they could reach a gauge factor close to 2 with CF-EP samples, as shown in **Figure 6b**.

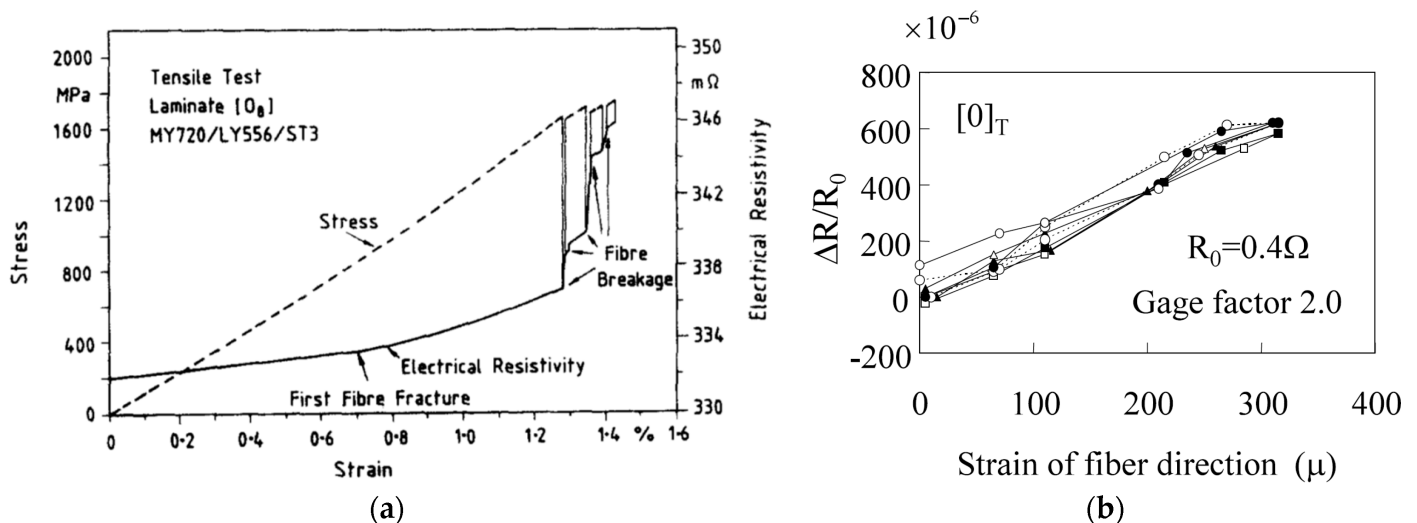


**Figure 6.** (a) Influence of strain on the resistance of a unidirectional Carbon fibre reinforced epoxy [46]. (b) Measured piezo-resistivity of a 0° CFRP sample during a tensile test [48].

### 3.2. Carbon Nanoparticles and Their Associated Nanocomposites as Self-Sensing Systems

To generate self-sensing composites from electrical insulating components, the most common way is to integrate conductive particles into the insulating matrix. CNT are thus good candidates thanks to their high electrical, mechanical, thermal, optical properties, and large aspect ratio [50][51][52][53][54][55].

#### 3.2.1. Electrical Behaviour of CNT-Filled Polymer: Theory of Statistic Percolation

The electrical conductivity of nanocomposites is obtained through the dispersion of conductive fillers into an insulating matrix. Increasing the amount of conductive fillers leads to an insulator-to-conductor transition, as illustrated in **Figure 7**. At low content of fillers dispersed in a matrix, no conductive pathway can be created

inducing an insulating electrical behaviour [56]. When the first conductive pathway appears throughout the material, an insulator-to-conductor transition occurs with a sudden decrease of the material's resistivity [57][58]. This sharp transition is commonly referred as the percolation threshold. Above the percolation threshold, the matrix conductivity can be described by the Equation [59]:

$$\rho = \rho_0(\varphi - \varphi_c)^{-t}$$

where  $\varphi$  indicates the volume fraction of the conductive filler,  $\varphi_c$  the volume fraction at the percolation threshold,  $\rho$  and  $\rho_0$  are the resistivity at  $\varphi$  and for an infinite content of filler respectively,  $t$  is the critical exponent comprises between 1.3 and 2.0.

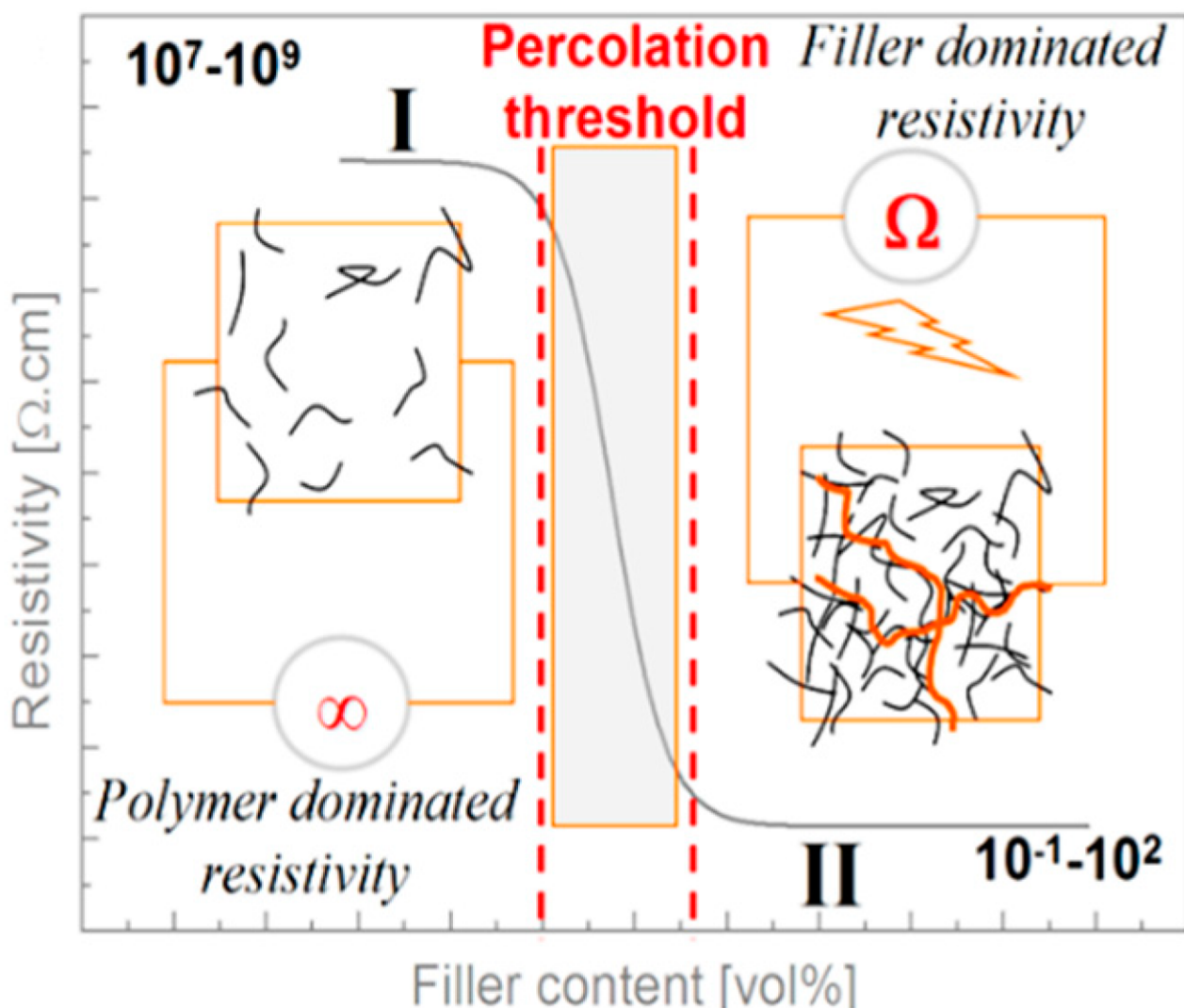


**Figure 7.** Resistivity behaviour of a polymer with the increase of filler volume content. The left inset, in region I, represents the fillers dispersion with no conductive pathway and a resulting nearly infinite resistivity. The central zone depicts the insulator-to-conductor transition with the formation of the first conductive path. The right inset, in

region II, represents the fillers dispersion in a conductive matrix with several electrical pathways, resulting in low electrical resistance [60].

### 3.2.2. Bucky Paper as a Strain Sensing Element

Dharap et al. [15][61][62] were the first to use the electrical properties of CNT to develop a strain sensing device. They used a pure SWCNT film called Bucky paper (BP). The film was glued on the surface of a brass sample by a PVC film and epoxy. It allowed them to choose BP dimension and location and to use it as a strain sensor. The response of the film's voltage, obtained by a four-point probe method, as a function of the specimen strain was linear.

The capability of BP to detect defects and damages has also been investigated. Indeed, the propagation of a delamination through the BP would break the CNT network, and therefore enhanced the resistance drastically as shown in **Figure 8**. The resistance was multiplied by 5 after 500 MPa in the propagation stage (II) compared to the undamaged stage (I) [63]. While monitoring the fracture, the BP electrical resistance was found to be noisy and increasing until infinite value in the fracture stage (III).

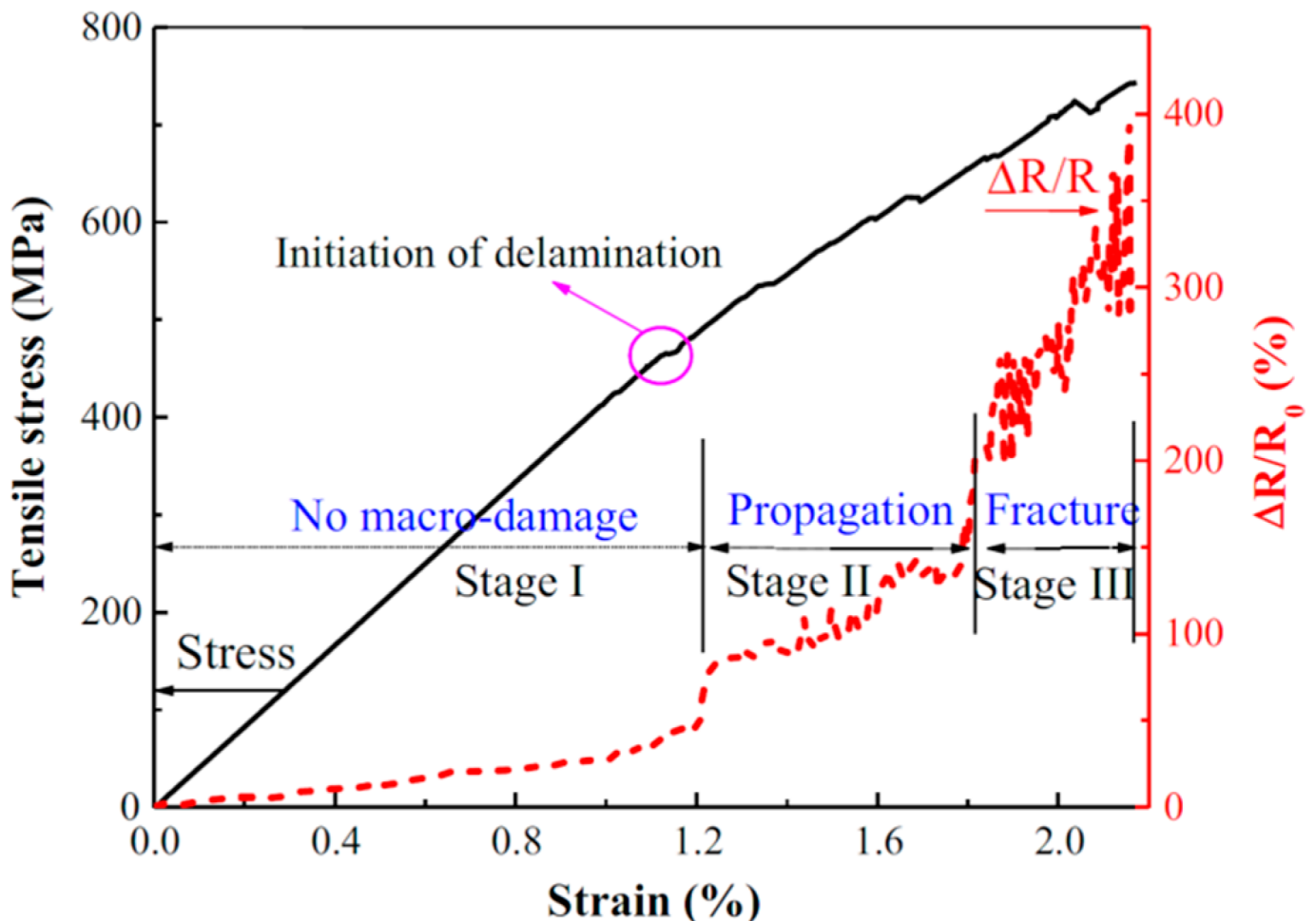


**Figure 8.** The completed stress–strain and corresponding  $\Delta R/R_0\%$  response curve for a CNT BP embedded in a CFEP. Three areas are visible: the stage I until 500 MPa where no macro-damage occurs, the stage II until 600

MPa corresponding to the propagation of damage after the first appearance, and stage III with the final fracture [63].

### 3.2.3. CNT Dispersed in a Matrix as a Sensing Element

#### Sensing with a CNT Nanocomposite Matrix

A second possibility of preparing self-sensing materials was proposed by Fiedler et al. [64] in 2004. They introduced nanotubes inside the composite epoxy matrix to create a percolated network. Therefore, the whole matrix (and thus the whole composite part) became an electrically sensing element, in which strain would induce a network change and consequently a change of its resistance. Thostenson et al. [65][66][67][68][69][70][71][72][73][74] added 0.5 wt % of MWCNT into the resin of a glass fibre epoxy (GF-EP) laminate and monitored real-time strain applied to the composite. They linked the changes in the resistance's slope with strain to the composite intrinsic events. **Figure 9a** presents the electrical behaviour when the laminate is subjected to increasing cycling loading. Three electrical behaviours have been associated to specific events, i. e. the opening of previous cracks, the elastic deformation of the sample, and the accumulation of new damage in the laminate. Further related this accumulation of damage to the drift of resistance at rest is shown in **Figure 9b**.

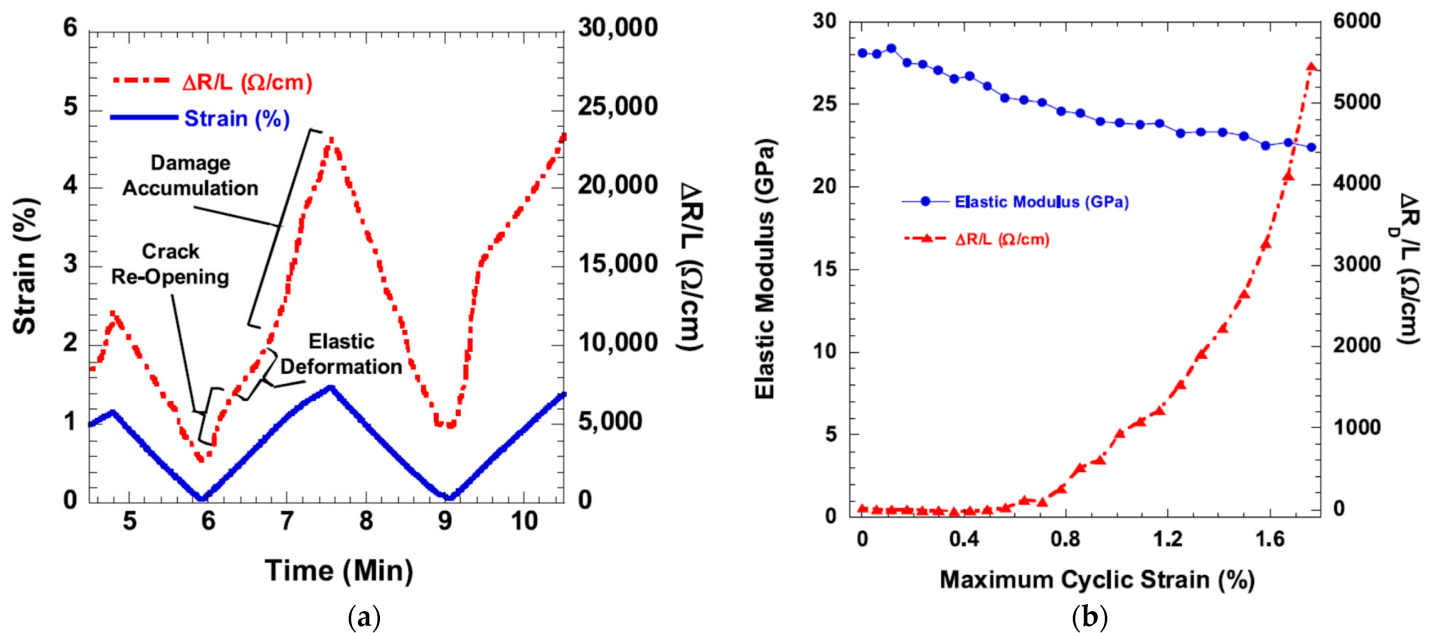


**Figure 9.** (a) Cyclic loading of a cross-ply glass fibre CNT-epoxy laminate showing resistance and strain response. During the tensile part, three electrical behaviours are noticeable by the change of slope: crack reopening, elastic deformation and damage accumulation [72]. (b) Evolution with the cyclic loading of the elastic modulus and resistance at rest due the damage in a cross-ply glass fibre CNT-epoxy laminate [72].

#### Sensing with a Patch of CNT Nanocomposites

Instead of dispersing CNT in the whole sample matrix, the alternative solution of introducing locally a patch of matrix-CNT nanocomposite has been studied. This local sensor could be deposited on the surface of the composite specimen by resin casting [75][76], spraying [77] as shown in **Figure 10** (left), or printing [78][79][80][81]. The

ply is inserted prior the epoxy infusion process, thus after fabrication, the sensors are embedded in the sample's core **Figure 10** (right). The sensor's sensitivity can be furthermore adjusted with the filler content in the matrix according to the percolation law [82]. The use of an epoxy-CNT nanocomposite, closely above its percolation threshold at 0.5 wt %, allowed reaching a very high GF value of 78 [80], while at 0.7 wt % the GF was about 3.2 [75]. Such sensors have a typical thickness ranging from 1  $\mu\text{m}$  [77] to 100  $\mu\text{m}$  [75]. Michelis et al. [83] also proposed a CNT based strain gauge made by inkjet printing of CNT on a polymer substrate that allowed them to make a strain gauge with a GF of 0.98. A similar process has been used by Kaiyan et al. [84] with the addition of epoxy in the sensor, reaching a GF of 50 and 20 for 0.3 and 0.5 wt % CNT composite, respectively. Nevertheless, one could argue that the sensor is still located on the surface of the sample, which avoids in situ core measurements. As for other industrial sensors, this sensor would also be affected by moisture and temperature. Another strategy is to embed the CNT based epoxy sensor in the core of the structure. Feller et al. [85][82] have sprayed layer by layer (sLbL) CNT-epoxy solutions on the dry glass fibres from the reinforcement textile prior to epoxy infusion and final curing of the composite, as illustrated in **Figure 10**.

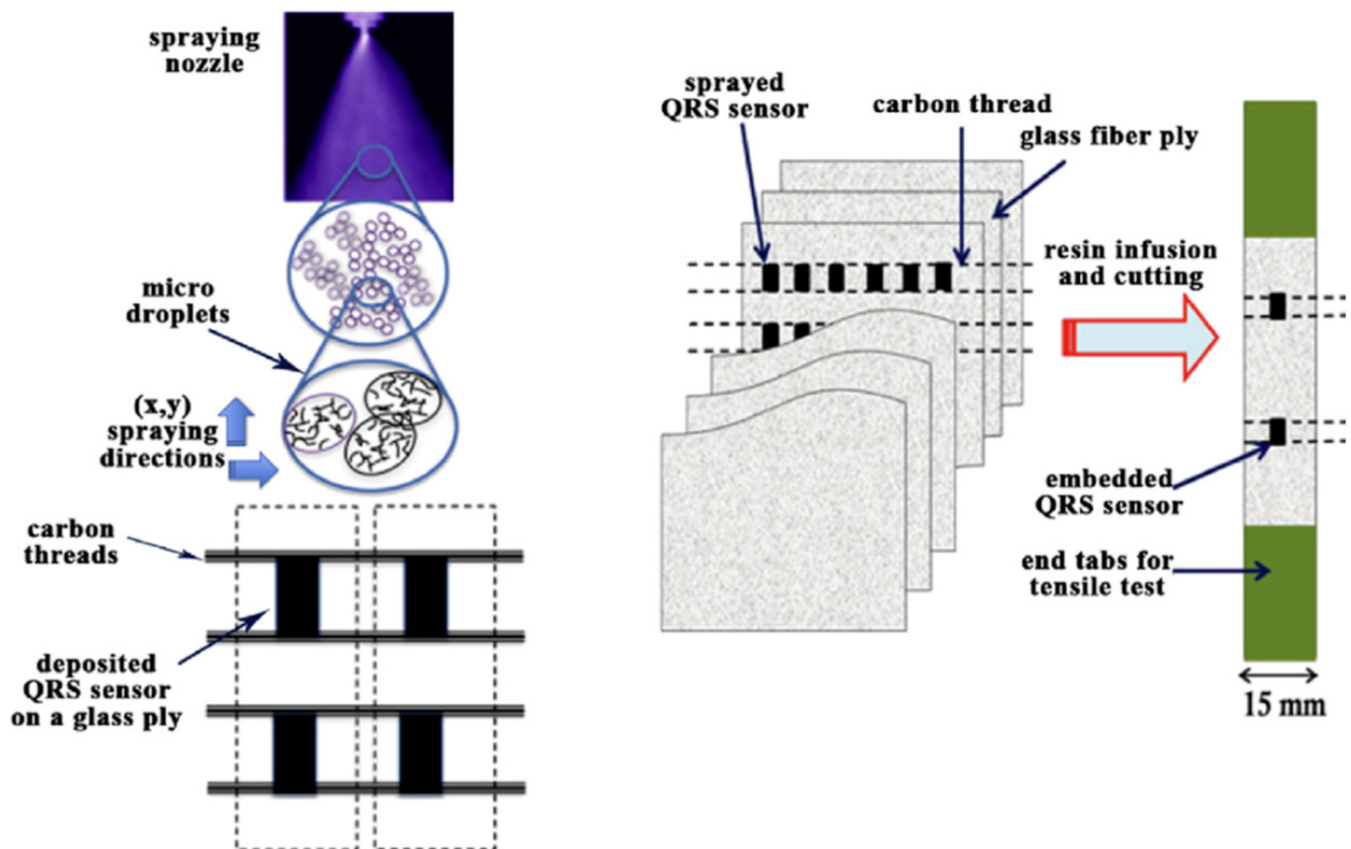
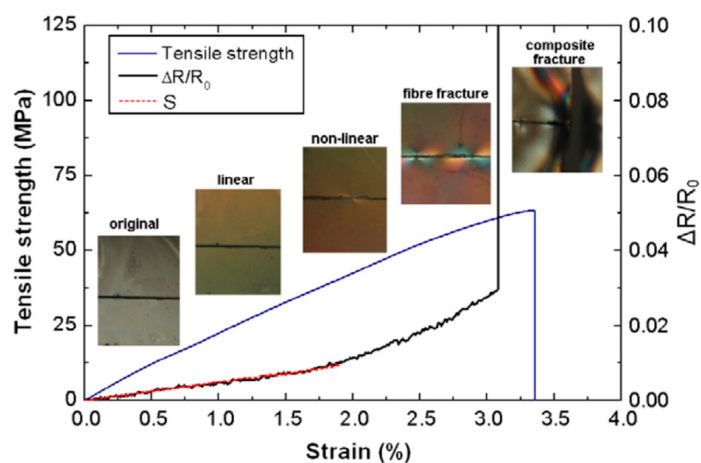


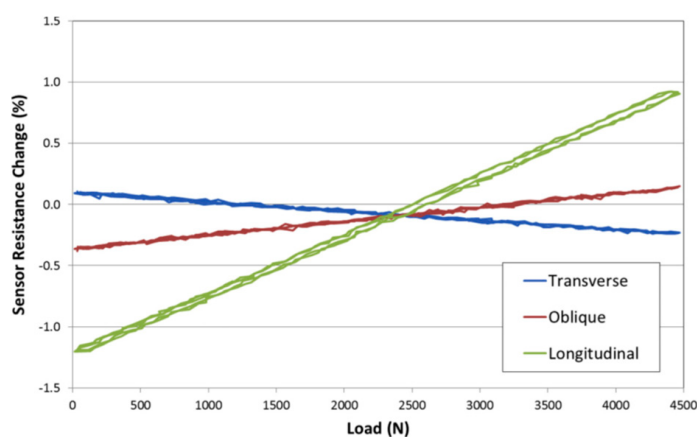
**Figure 10.** Fabrication steps of composite samples equipped with two embedded sprayed nanocomposites sQRS. A liquid solution containing the epoxy-CNT mixture is sprayed layer by layer directly on the glass fibre fabric (left). The ply is inserted prior the epoxy infusion process. Thus, after fabrication, the sensors are embedded in the sample's core (right) [82].

### 3.2.4. CNT Coated Reinforcing Fibres as a Sensing Element

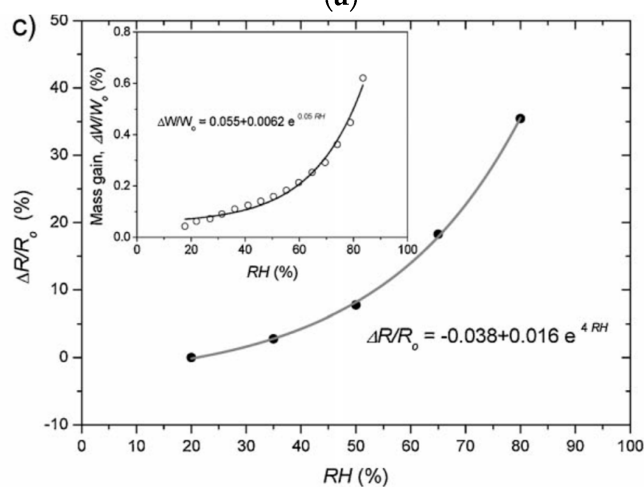
Another way to trigger the sensitivity of a composite has been investigated in the literature through the coating of fibres with CNT, later on inserted in the laminate, thus called “fuzzy fibre”. Zhang et al. [86] showed that this strategy allowed the monitoring of the piezo-resistive behaviour at the interface between a single fuzzy fibre and the polymer matrix. Mäder et al. [87][88][89][90] made the surface of glass fibres conductive by electrophoretic deposition (EPD) [91] and dip-coating in a nanotubes solution prior to embedding it into an epoxy matrix. The scholars performed tensile deformation on the laminate with an in-situ electrical measurement, as shown in **Figure 11a**, and identified three stages in the electrical response. At first, the resistance variation was linear with the applied strain, as caused by dimensional changes of MWCNT network in the interphase. At 1% of strain, they measured a GF close to 1. Then, an exponentially increase of the slope was observed. The scholars related it to the stress concentration at interphases, the increasing distance between CNT and the loss of contact points. Finally, the propagation of cracks in the composite disconnected the network, inducing the resistance value to suddenly increase to infinite. In this way, the scholars suggested that CNT coated glass fibre could be used as a mechanical sensor, and this CNT-fibre architecture has ensued interest in the fibres manufacturer community [92]. The scholars have also investigated the use of a CNT network as a temperature and humidity sensor as shown in **Figure 11c,d** [88]. They found an exponential relation with humidity, i.e., the resistance was increased by 50% from 20 to 80 RH %.



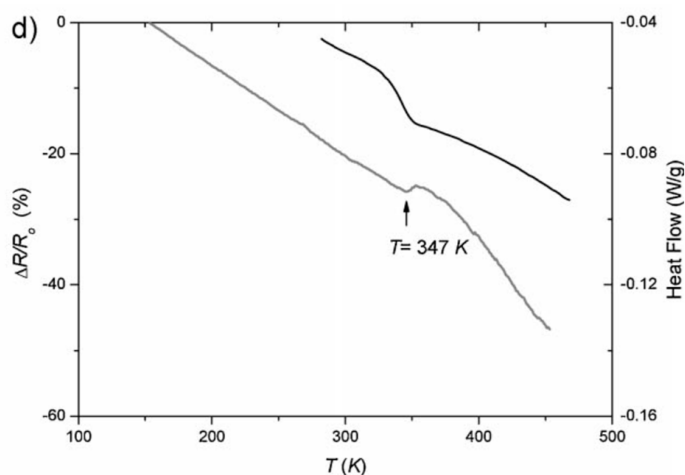
(a)



(b)



(c)



(d)

**Figure 11.** (a) Simultaneous change of electrical resistance and stress as a function of strain for single coated fibre/epoxy composite. Inset figures correspond to the sample profiles at different stages [87]. (b) Fuzzy fibre's resistance variation with load for different orientations [93]. Relative (c) humidity and (d) temperature dependence of a fuzzy fibre [88].

### 3.2.5. Self-Sensing Materials Based on Hybrid Fillers

Besides CNT, others nano-carbon based fillers have been studied to tune the electrical properties of insulating composites, like carbon nanoparticles (CNP), graphite and graphene nano-platelets (GNP), as shown in **Figure 12**. CNP are nearly spherical particles from 10 to 100 nm welded together during their synthesis into aggregates of 200 to 800 nm [94]. GNP are planar sheets about 1 nm thick and several micron length [95]. CNT are made of graphene sheets shaped into the form of a tube with one to 20 walls. For commercial multi-walled CNT, the external diameter and the length are about 10 nm and 1  $\mu\text{m}$  respectively [96]. As for CNT, those carbon-based fillers can also be used to improve the mechanical [97][98][99][100], thermal [99][100][101][102], or electrical properties of nanocomposites [76][94][103][104][105][106][107][108][109] and often led to modified rheological [110][111] and crystallization behaviours [112][113].

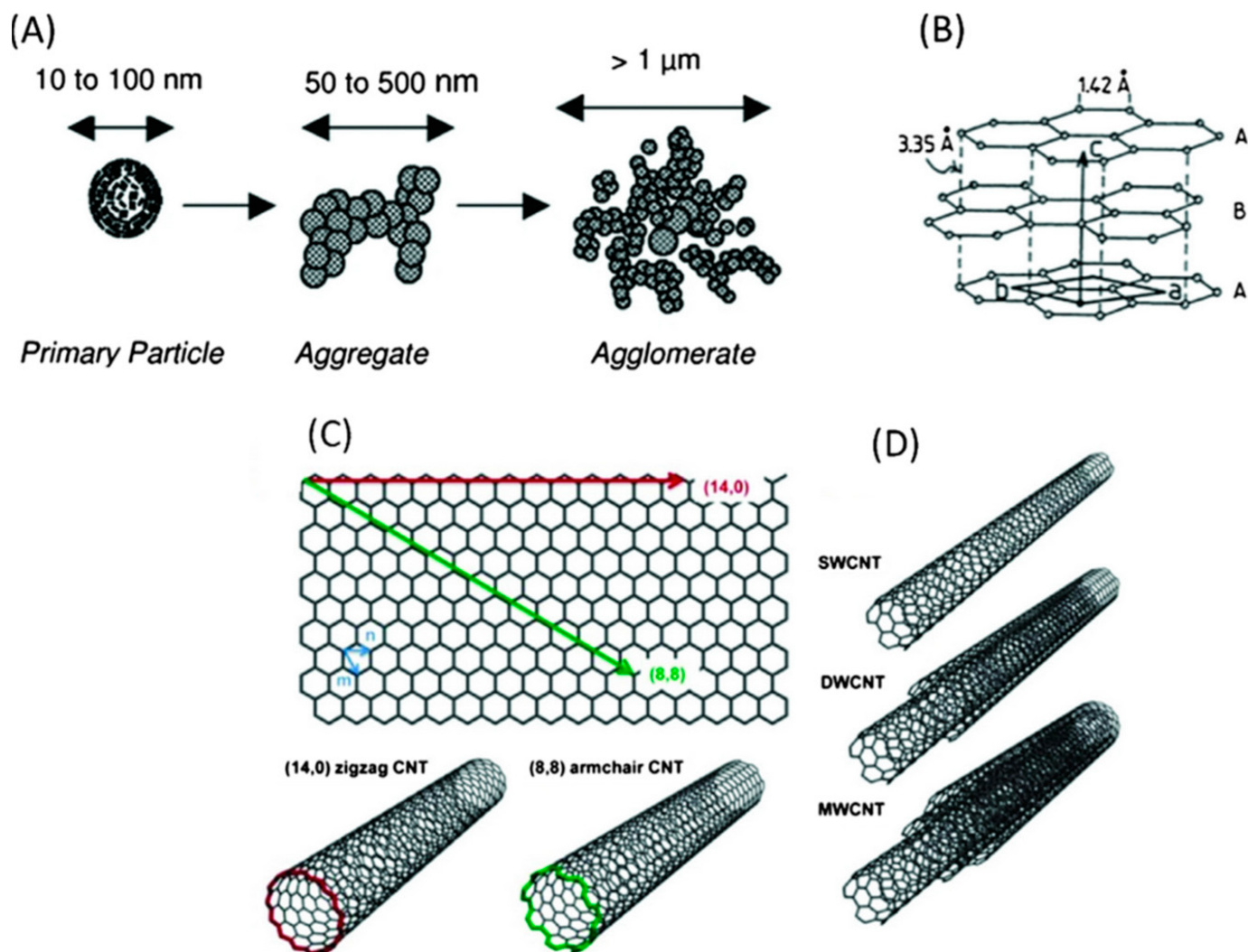


**Figure 12.** Schematic structure of (A) carbon black primary particles fused together to form aggregates and agglomerates; (B) hexagonal graphite showing the ABAB stacking of honeycomb carbon layers; (C) structural variety of CNT and orientation of the carbon network in armchair ( $n, n$ ) and zigzag configuration ( $n, 0$ ); (D) Single, double and multi-walled CNT [\[114\]](#).

## 4. Conclusions

The creation of conductive networks inside the insulating epoxy matrix by the percolation of nano carbon fillers, especially CNT, seemed the most promising. The simple monitoring of the nano composite's resistance allows to correlate strain and damage with the matrix piezo-resistive behaviour. However, the state of dispersion, as well as the CNT content in the matrix appear to be primordial parameters to control, in order to obtain nanocomposite strain sensors with reproducible performances.

Three approaches have been discussed for different kind of CNT networks: Bucky paper (random network of CNT), matrix reinforcement (CNT percolated into the polymer) and fuzzy fibres (CNT coating an insulating fibre). All strategies proved to be effective in measuring strain and detecting damages. Nevertheless, some lockers to their industrialisation remain, such as for instance, the weakening of the interface between the CNT and the matrix resulting from the use of Bucky papers that may decrease the composite mechanical properties.

While, the localisation of strain and damage in a matrix completely filled with CNT has been demonstrated with both ERT and EPM technics, a reduction of the calculation time (ERT) or the number of electrodes (EPM) should still be improved for real time monitoring and some issues remain for their insertion in the core of parts. In the case of fuzzy fibres, a sensitivity to the orientation of strain can be obtained thanks to the high aspect ratio of fibres.

Finally, the possible synergistic effect between carbon nanofillers in epoxy-based hybrid composites has been confirmed to optimize their electrical behaviour. Thanks to the different particles' geometry the bridging effect and the creation of hub like interconnection can enhance specific electrical parameters such stability of responses during cyclic deformation, partial disappearance of double peaks in compression due to the Poisson's effect.

The state of the art on existing structural health monitoring (SHM) for turbine blades made of composite structures has allowed to list the different techniques used: metallic strain gauge and optical fibres for strain measurement, and acoustic emission, ultrasonic measurements and optical fibres for failure analysis. Among these technics, only optical fibres can detect both strain and failure, but their use for in situ measurements in the core of composites is still controversial, as their handling during processing is tricky and their integration susceptible to weaken the composite depending on the structure of its plies.

Consequently, the development of "self-sensing" composites appears to provide a credible alternative to overcome those issues. Actually, these materials proved to be able to give a real-time information about their mechanical behaviour and their environment. By simply analysing the resistance variations of their carbon network, it is possible to evidence delamination, fibre's fracture, and eventually locate structural defects.

Future development of self-sensing sensors will certainly include hybrid nanocomposites obtained by the combination of various nano carbon fillers such as CNP, CNT, or graphene, which proved a synergistic effect able to enhance their sensitivity and stabilize their signals.

However, an increase of the technological readiness level (TRL) of piezo-resistive nanocomposite sensors for structural health monitoring (SHM) still requires the implementation in the data treatment, of the influence of environmental parameters such as temperature and moisture for example. It is also likely that the massive acquisition of data in use conditions and their fusion with data from other classical surface technics like acoustic emission (AE), will allow to perform sharper diagnostics.

---

## References

1. Schubel, P.J.; Crossley, R.J.; Boateng, E.K.G.; Hutchinson, J.R. Review of structural health and cure monitoring techniques for large wind turbine blades. *Renew. Energy* 2013, 51, 113–123.
2. Balageas, D.; Fritzen, C.-P.; Güemes, A. *Structural Health Monitoring*; ISTE: Newport Beach, CA, USA, 2006; ISBN 978-1-905209-01-9.
3. Huston, D. *Structural Sensing, Health Monitoring, and Performance Evaluation (Series in Sensors)*; CRC Press: Boca Raton, FL, USA, 2011; ISBN 9781420012354.
4. Farrar, C.R.; Worden, K. An introduction to structural health monitoring. *Philos. Trans. R. Soc. A Math. Phys. Eng. Sci.* 2007, 365, 303–315.
5. Castro-Santos, L.; Diaz-Casas, V. *Green Energy and Technology*. In *Floating Offshore Wind Farms*; Castro-Santos, L., Diaz-Casas, V., Eds.; Springer International Publishing: Cham, Germany, 2016; ISBN 978-3-319-27970-1.
6. McGugan, M.; Ostachowicz, W.; Schröder-Hinrichs, J.-U.; Luczak, M. *Mare-Wint*; Ostachowicz, W., McGugan, M., Schröder-Hinrichs, J.-U., Luczak, M., Eds.; Springer International Publishing: Cham, Germany, 2016; ISBN 978-3-319-39094-9.
7. Sørensen, B.F.; Jørgensen, E.; Debel, C.P.; Jensen, F.M.; Jensen, H.M.; Jacobsen, T.K.; Halling, K.M. *Improved Design of Large Wind Turbine Blade of Fibre Composites Based on Studies of Scale Effects (Phase 1)—Summary Report*; Risø-R-139: Roskilde, Denmark, 2004; Volume 1390, ISBN 87-550-3176-5/87-550-3177-3.
8. Chen, X.; Zhao, X.; Xu, J. Revisiting the structural collapse of a 52.3 m composite wind turbine blade in a full-scale bending test. *Wind Energy* 2017, 20, 1111–1127.
9. Dransfield, K.; Baillie, C.; Mai, Y.-W. Improving the delamination resistance of CFRP by stitching—a review. *Compos. Sci. Technol.* 1994, 50, 305–317.

10. Takoutsing, P.; Wamkeue, R.; Ouhrouche, M.; Slaoui-Hasnaoui, F.; Tameghe, T.; Ekemb, G. Wind turbine condition monitoring: State-of-the-art review, new trends, and future challenges. *Energies* 2014, 7, 2595–2630.
11. Cooperman, A.; Martinez, M. Load monitoring for active control of wind turbines. *Renew. Sustain. Energy Rev.* 2015, 41, 189–201.
12. Hameed, Z.; Hong, Y.S.; Cho, Y.M.; Ahn, S.H.; Song, C.K. Condition monitoring and fault detection of wind turbines and related algorithms: A review. *Renew. Sustain. Energy Rev.* 2009, 13, 1–39.
13. Hoffmann, K. An Introduction to Stress Analysis and Transducer Design using Strain Gauges. *Academia* 2012, 127–133.
14. Nanolike, Monitor Your Industrial Assets. Available online: <http://www.nanolike.com/> (accessed on 25 November 2021).
15. Dharap, P.; Li, Z.; Nagarajaiah, S.; Barrera, E.V. Nanotube film based on single-wall carbon nanotubes for strain sensing. *Nanotechnology* 2004, 15, 379–382.
16. Eisler, P. Electric Resistance Devices. US Patent US2441960A, 1952. Available online: <https://patents.google.com/patent/US2441960A/en> (accessed on 25 November 2021).
17. Rs Components. Available online: <http://fr.rs-online.com/web/c/automatisme-et-contrôle-de-process/capteurs-et-transducteurs/jauges-de-contraintes/> (accessed on 25 November 2021).
18. Majumder, M.; Gangopadhyay, T.K.; Chakraborty, A.K.; Dasgupta, K.; Bhattacharya, D.K. Fibre Bragg gratings in structural health monitoring—Present status and applications. *Sens. Actuators A Phys.* 2008, 147, 150–164.
19. Li, H.-N.; Li, D.-S.; Song, G.-B. Recent applications of fiber optic sensors to health monitoring in civil engineering. *Eng. Struct.* 2004, 26, 1647–1657.
20. Ramakrishnan, M.; Rajan, G.; Semenova, Y.; Farrell, G. Overview of fiber optic sensor technologies for strain/temperature sensing applications in composite materials. *Sensors* 2016, 16, 99.
21. Takeda, N. Characterization of microscopic damage in composite laminates and real-time monitoring by embedded optical fiber sensors. *Int. J. Fatigue* 2002, 24, 281–289.
22. Takeda, N.; Okabe, Y.; Kuwahara, J.; Kojima, S.; Ogisu, T. Development of smart composite structures with small-diameter fiber Bragg grating sensors for damage detection: Quantitative evaluation of delamination length in CFRP laminates using Lamb wave sensing. *Compos. Sci. Technol.* 2005, 65, 2575–2587.
23. Li, C.; Ning, T.; Li, J.; Pei, L.; Zhang, C.; Zhang, C.; Lin, H.; Wen, X. Simultaneous measurement of refractive index, strain, and temperature based on a four-core fiber combined with a fiber Bragg

- grating. *Opt. Laser Technol.* 2017, 90, 179–184.
24. Mieloszyk, M.; Ostachowicz, W. Moisture contamination detection in adhesive bond using embedded FBG sensors. *Mech. Syst. Signal Process.* 2017, 84, 1–14.
  25. Mieloszyk, M.; Ostachowicz, W. An application of Structural Health Monitoring system based on FBG sensors to offshore wind turbine support structure model. *Mar. Struct.* 2017, 51, 65–86.
  26. Kinet, D.; Mégret, P.; Goossen, K.; Qiu, L.; Heider, D.; Caucheteur, C. Fiber Bragg grating sensors toward structural health monitoring in composite materials: Challenges and solutions. *Sensors* 2014, 14, 7394–7419.
  27. Huang, C.Y.; Trask, R.S.; Bond, I.P. Characterization and analysis of carbon fibre-reinforced polymer composite laminates with embedded circular vasculature. *J. R. Soc. Interface* 2010, 7, 1229–1241.
  28. Luyckx, G.; Voet, E.; Lammens, N.; Degrieck, J. Strain measurements of composite laminates with embedded fibre Bragg gratings: Criticism and opportunities for research. *Sensors* 2010, 11, 384–408.
  29. Yang, R.; He, Y.; Zhang, H. Progress and trends in non-destructive testing and evaluation for wind turbine composite blade. *Renew. Sustain. Energy Rev.* 2016, 60, 1225–1250.
  30. Juengert, A. Damage Detection in Wind Turbine Blades using two Different Acoustic Techniques. *E-J. Nondestruct. Test.* 2008, 1–10. Available online: <https://www.ndt.net/article/v13n12/juengert.pdf> (accessed on 25 November 2021).
  31. García Márquez, F.P.; Tobias, A.M.; Pinar Pérez, J.M.; Papaelias, M. Condition monitoring of wind turbines: Techniques and methods. *Renew. Energy* 2012, 46, 169–178.
  32. Beganovic, N.; Söffker, D. Structural health management utilization for lifetime prognosis and advanced control strategy deployment of wind turbines: An overview and outlook concerning actual methods, tools, and obtained results. *Renew. Sustain. Energy Rev.* 2016, 64, 68–83.
  33. Ciang, C.C.; Lee, J.-R.; Bang, H.-J. Structural health monitoring for a wind turbine system: A review of damage detection methods. *Meas. Sci. Technol.* 2008, 19, 122001.
  34. Signaltech, Capteurs d'émission Acoustique. Available online: <http://www.signaltech.fr/capteurs/emisacoust.html> (accessed on 25 November 2021).
  35. Juengert, A.; Grosse, C.U. Inspection techniques for wind turbine blades using ultrasound and sound waves. In *Proceedings of the NDTCE'09, Non-Destructive Testing in Civil Engineering*, Nantes, France, 30 June–3 July 2009.
  36. John, W.N. Method and Apparatus for Monitoring Wind Turbine Blades during Operation. 2013. Available online: <https://patents.google.com/patent/US9194843B2/en> (accessed on 25 November 2021).

37. John, W.N. Nondestructive Testing of Wind Turbine Blades from the Ground during Operation. 2014. Available online: <https://patentimages.storage.googleapis.com/09/64/e0/226b5cebac2bb6/EP2984337B1.pdf> (accessed on 25 November 2021).
38. Frey, A.; Roark, F.; Gonzalez, M. Early Detection of Wind Turbine Degradation Using Acoustical Monitoring. 2013. Available online: <https://patentimages.storage.googleapis.com/2c/49/e6/83c174d186ad4d/CA2891326A1.pdf> (accessed on 25 November 2021).
39. Method and Apparatus for Monitoring Wind Turbine Blades during Operation. US Patent US2014260634A1, 2014. Available online: <https://patents.google.com/patent/US20140260634?q=2014260634A1> (accessed on 25 November 2021).
40. Raišutis, R.; Jasi, E.; Šliteris, R.; Vladišauskas, A.; Jasiūnienė, E.; Šliteris, R.; Vladišauskas, A. The review of non-destructive testing techniques suitable for inspection of the wind turbine blades. *Ultragarsas* 2008, 63, 26–30.
41. Giurgiutiu, V. 7.19 Smart Materials and Health Monitoring of Composites. In *Comprehensive Composite Materials II*; Beaumont, P.W.R., Zweben, C.H., Eds.; Elsevier: Amsterdam, The Netherlands, 2018; pp. 364–381. ISBN 9780128035818.
42. Wind Turbine Blade with Strain Sensing Means, Wind Turbine Block Sensor Unit and Uses Hereof. WO Patent WO2008101496A3, 2011. Available online: <https://patents.google.com/patent/WO2008101496A3/en> (accessed on 25 November 2021).
43. Tan, K.T.; Watanabe, N.; Iwahori, Y. X-ray radiography and micro-computed tomography examination of damage characteristics in stitched composites subjected to impact loading. *Compos. B Eng.* 2011, 42, 874–884.
44. Schell, J.S.U.; Renggli, M.; van Lenthe, G.H.; Müller, R.; Ermanni, P. Micro-computed tomography determination of glass fibre reinforced polymer meso-structure. *Compos. Sci. Technol.* 2006, 66, 2016–2022.
45. Hofer, B. Fibre optic damage detection in composite structures. *Composites* 1987, 18, 309–316.
46. Schulte, K.; Baron, C. Load and failure analyses of CFRP laminates by means of electrical resistivity measurements. *Compos. Sci. Technol.* 1989, 36, 63–76.
47. Wang, X.; Chung, D.D.L. Short-carbon-fiber-reinforced epoxy as a piezoresistive strain sensor. *Smart Mater. Struct.* 1995, 4, 363–367.
48. Todoroki, A.; Yoshida, J. Electrical resistance change of unidirectional CFRP due to applied load. *JSME Int. J. Ser. A* 2004, 47, 357–364.

49. Todoroki, A.; Ueda, M.; Hirano, Y. Strain and damage monitoring of CFRP laminates by means of electrical resistance measurement. *J. Solid Mech. Mater. Eng.* 2007, 1, 947–974.
50. Thostenson, E.T.; Ren, Z.; Chou, T.W. Advances in the science and technology of carbon nanotubes and their composites: A review. *Compos. Sci. Technol.* 2001, 61, 1899–1912.
51. Kim, P.; Shi, L.; Majumdar, A.; McEuen, P.L. Thermal Transport Measurements of Individual Multiwalled Nanotubes. *Phys. Rev. Lett.* 2001, 87, 215502.
52. Asai, S.; Sumita, M. Effect of interfacial energy and viscosity on percolation time of carbon black-filled poly(methyl methacrylate). *J. Macromol. Sci. Part B* 1995, 34, 283–294.
53. Yao, Z.; Kane, C.L.; Dekker, C. High-Field Electrical Transport in Single-Wall Carbon Nanotubes. *Phys. Rev. Lett.* 2000, 84, 2941–2944.
54. Ebbesen, T.W.; Lezec, H.J.; Hiura, H.; Bennett, J.W.; Ghaemi, H.F.; Thio, T. Electrical conductivity of individual carbon nanotubes. *Nature* 1996, 382, 54–56.
55. Treacy, M.M.J.; Ebbesen, T.W.; Gibson, J.M. Exceptionally high Young's modulus observed for individual carbon nanotubes. *Nature* 1996, 381, 678–680.
56. Feller, J.F.; Kumar, B.; Castro, M. Conductive biopolymer nanocomposites for sensors. In *Nanocomposites with Biodegradable Polymers: Synthesis, Properties & Future Perspectives*; Mital, V., Ed.; Oxford University Press: Oxford, UK, 2011; pp. 368–399. ISBN 978-0-19-958192-4.
57. Martin, C.A.; Sandler, J.K.W.; Shaffer, M.S.P.; Schwarz, M.K.; Bauhofer, W.; Schulte, K.; Windle, A.H. Formation of percolating networks in multi-wall carbon-nanotube–epoxy composites. *Compos. Sci. Technol.* 2004, 64, 2309–2316.
58. Ambrosetti, G.; Grimaldi, C.; Balberg, I.; Maeder, T.; Danani, A.; Ryser, P. Solution of the tunneling-percolation problem in the nanocomposite regime. *Phys. Rev. B* 2010, 81, 155434.
59. Stauffer, D.; Aharony, A. *Introduction to Percolation Theory*; Taylor & Francis: Abingdon-on-Thame, UK, 1994; Volume 6, ISBN 1420074792.
60. Feller, J.F.; Castro, M.; Kumar, B. Polymer-carbon nanotube conductive nanocomposites for sensing. In *Polymer-Carbon Nanotube Composites: Preparation, Properties & Applications*; McNally, T., Pötschke, P., Eds.; Woodhead Publishing Limited: Swaston, UK, 2011; pp. 760–803. ISBN 9781845697617.
61. Li, Z.; Dharap, P.; Nagarajaiah, S.; Barrera, E.V.; Kim, J.D. Carbon Nanotube Film Sensors. *Adv. Mater.* 2004, 16, 640–643.
62. Barrera, E.V.; Nagarajaiah, S.; Dharap, P.; Zhiling, L.; Kim, J.D. *Smart Materials: Strain Sensing and Stress Determination by Means of Nanotube Sensing Systems, Composites, and Devices*. 2010. Available online:

<https://patentimages.storage.googleapis.com/86/cd/4e/901c7b0b2dc158/US7730547.pdf>  
(accessed on 25 November 2021).

63. Liu, L.; Wu, J.; Zhou, Y. Enhanced delamination initiation stress and monitoring sensitivity of quasi-isotropic laminates under in-plane tension by interleaving with CNT buckypaper. *Compos. Part A Appl. Sci. Manuf.* 2016, 89, 10–17.
64. Fiedler, B.; Gojny, F.H.; Wichmann, M.H.G.; Bauhofer, W.; Schulte, K. Can carbon nanotubes be used to sense damage in composites? *Ann. Chim. Sci. Matériaux* 2004, 29, 81–94.
65. Li, C.; Thostenson, E.T.; Chou, T.W. Dominant role of tunneling resistance in the electrical conductivity of carbon nanotube-based composites. *Appl. Phys. Lett.* 2007, 91, 223114.
66. Thostenson, E.T.; Chou, T.W. Processing-structure-multi-functional property relationship in carbon nanotube/epoxy composites. *Carbon* 2006, 44, 3022–3029.
67. Gao, L.; Chou, T.W.; Thostenson, E.T.; Zhang, Z.; Coulaud, M. In situ sensing of impact damage in epoxy/glass fiber composites using percolating carbon nanotube networks. *Carbon* 2011, 49, 3382–3385.
68. Gao, L.; Chou, T.W.; Thostenson, E.T.; Zhang, Z. A comparative study of damage sensing in fiber composites using uniformly and non-uniformly dispersed carbon nanotubes. *Carbon* 2010, 48, 3788–3794.
69. Li, C.; Chou, T.W. Modeling of damage sensing in fiber composites using carbon nanotube networks. *Compos. Sci. Technol.* 2008, 68, 3373–3379.
70. Ahmed, S.; Doshi, S.; Schumacher, T.; Thostenson, E.T.; McConnell, J. Development of a novel integrated strengthening and sensing methodology for steel structures using CNT-based composites. *J. Struct. Eng.* 2017, 143, 04016202.
71. Thostenson, E.T.; Chou, T.W. Carbon nanotube-based health monitoring of mechanically fastened composite joints. *Compos. Sci. Technol.* 2008, 68, 2557–2561.
72. Thostenson, E.T.; Chou, T.W. Real-time in situ sensing of damage evolution in advanced fiber composites using carbon nanotube networks. *Nanotechnology* 2008, 19, 215713.
73. Gao, L.; Thostenson, E.T.; Zhang, Z.; Chou, T.W. Sensing of damage mechanisms in fiber-reinforced composites under cyclic loading using carbon nanotubes. *Adv. Funct. Mater.* 2009, 19, 123–130.
74. Gao, L.; Thostenson, E.T.; Zhang, Z.; Chou, T.W. Coupled carbon nanotube network and acoustic emission monitoring for sensing of damage development in composites. *Carbon* 2009, 47, 1381–1388.
75. Meeuw, H.; Viets, C.; Liebig, W.V.; Schulte, K.; Fiedler, B. Morphological influence of carbon nanofillers on the piezoresistive response of carbon nanoparticle/epoxy composites under

- mechanical load. *Eur. Polym. J.* 2016, 85, 198–210.
76. Chiacchiarelli, L.M.; Rallini, M.; Monti, M.; Puglia, D.; Kenny, J.M.; Torre, L. The role of irreversible and reversible phenomena in the piezoresistive behavior of graphene epoxy nanocomposites applied to structural health monitoring. *Compos. Sci. Technol.* 2013, 80, 73–79.
77. Robert, C.; Feller, J.F.; Castro, M. Sensing skin for strain monitoring made of PC-CNT conductive polymer nanocomposite sprayed layer by layer. *ACS Appl. Mater. Interfaces* 2012, 4, 3508–3516.
78. Sanli, A.; Müller, C.; Kanoun, O.; Elibol, C.; Wagner, M.F.X. Piezoresistive characterization of multi-walled carbon nanotube-epoxy based flexible strain sensitive films by impedance spectroscopy. *Compos. Sci. Technol.* 2016, 122, 18–26.
79. Kanoun, O.; Benchirouf, A.; Sanli, A.; Bouhamed, A.; Bu, L. Potential of Flexible Carbon Nanotube Films for High Performance Strain and Pressure Sensors. In *Nanotechnology for Optics and Sensors*; One Central Press: Altrincham, UK, 2014; pp. 148–183.
80. Sanli, A.; Benchirouf, A.; Müller, C.; Kanoun, O. Piezoresistive performance characterization of strain sensitive multi-walled carbon nanotube-epoxy nanocomposites. *Sens. Actuators A Phys.* 2017, 254, 61–68.
81. Bouhamed, A.; Müller, C.; Choura, S.; Kanoun, O. Processing and characterization of MWCNTs/epoxy nanocomposites thin films for strain sensing applications. *Sens. Actuators A Phys.* 2017, 257, 65–72.
82. Nag-Chowdhury, S.; Bellégou, H.; Pillin, I.; Castro, M.; Longrais, P.; Feller, J.F. Non-intrusive health monitoring of infused composites with embedded carbon quantum piezo-resistive sensors. *Compos. Sci. Technol.* 2016, 123, 286–294.
83. Michelis, F.; Bodelot, L.; Bonnassieux, Y.; Lebental, B. Highly reproducible, hysteresis-free, flexible strain sensors by inkjet printing of carbon nanotubes. *Carbon* 2015, 95, 1020–1026.
84. Kaiyan, H.; Weifeng, Y.; Shuying, T.; Haidong, L. A fabrication process to make CNT/EP composite strain sensors. *High Perform. Polym.* 2018, 30, 224–229.
85. Pillin, I.; Castro, M.; Nag-Chowdhury, S.; Feller, J.F. Robustness of carbon nanotube-based sensor to probe composites' interfacial damage in situ. *J. Compos. Mater.* 2016, 50, 109–113.
86. Zhang, H.; Bilotti, E.; Peijs, T. The use of carbon nanotubes for damage sensing and structural health monitoring in laminated composites: A review. *Nanocomposites* 2015, 1, 177–194.
87. Zhang, J.; Zhuang, R.; Liu, J.; Mäder, E.; Heinrich, G.; Gao, S. Functional interphases with multi-walled carbon nanotubes in glass fibre/epoxy composites. *Carbon* 2010, 48, 2273–2281.
88. Gao, S.L.; Zhuang, R.C.; Zhang, J.; Liu, J.W.; Mäder, E. Glass fibers with carbon nanotube networks as multifunctional sensors. *Adv. Funct. Mater.* 2010, 20, 1885–1893.

89. Siddiqui, N.A.; Li, E.L.; Sham, M.; Zhong, B.; Lin, S.; Mäder, E.; Kim, J. Tensile strength of glass fibres with carbon nanotube—epoxy nanocomposite coating: Effects of CNT morphology and dispersion state. *Compos. Part A* 2010, 41, 539–548.
90. Zhang, J.; Liu, J.; Zhuang, R.; Mäder, E.; Heinrich, G.; Gao, S. Single MWNT-Glass Fiber as Strain Sensor and Switch. *Adv. Mater.* 2011, 23, 3392–3397.
91. Sarkar, P.; Nicholson, P.S. Electrophoretic Deposition (EPD): Mechanisms, Kinetics, and Application to Ceramics. *J. Am. Ceram. Soc.* 1996, 79, 1987–2002.
92. Nguyen, F.N.; Yoshioka, K. Conductive Fiber Reinforced Polymer Composite and Multifunctional Composite. Patent n° TW201443120 (A), 11 October 2017.
93. Sebastian, J.; Schehl, N.; Bouchard, M.; Boehle, M.; Li, L.; Lagounov, A.; Lafdi, K. Health monitoring of structural composites with embedded carbon nanotube coated glass fiber sensors. *Carbon* 2014, 66, 191–200.
94. Accorsi, J.V. The Impact of Carbon Black Morphology and Dispersion on the Weatherability of polyethylene. *Kautsch. Gummi Kunstst.* 2001, 54, 321–326.
95. Available online: <http://www.angstrommaterials.com> (accessed on 25 November 2021).
96. Available online: <http://www.nanocyl.com> (accessed on 25 November 2021).
97. Frasca, D.; Schulze, D.; Wachtendorf, V.; Huth, C.; Schartel, B. Multifunctional multilayer graphene/elastomer nanocomposites. *Eur. Polym. J.* 2015, 71, 99–113.
98. Jia, J.; Du, X.; Chen, C.; Sun, X.; Mai, Y.; Kim, J. 3D network graphene interlayer for excellent interlaminar toughness and strength in fiber reinforced composites. *Carbon* 2015, 95, 978–986.
99. Yasmin, A.; Daniel, I.M. Mechanical and thermal properties of graphite platelet/epoxy composites. *Polymer* 2004, 45, 8211–8219.
100. Saleem, H.; Edathil, A.; Ncube, T.; Pokhrel, J.; Khoori, S.; Abraham, A.; Mittal, V. Mechanical and thermal properties of thermoset-graphene nanocomposites. *Macromol. Mater. Eng.* 2016, 301, 231–259.
101. Kumar, P.; Yu, S.; Shahzad, F.; Hong, S.M.; Kim, Y.-H.; Koo, C.M. Ultrahigh electrically and thermally conductive self-aligned graphene/polymer composites using large-area reduced graphene oxides. *Carbon* 2016, 101, 120–128.
102. Debelak, B.; Lafdi, K. Use of exfoliated graphite filler to enhance polymer physical properties. *Carbon* 2007, 45, 1727–1734.
103. Shen, J.T.; Buschhorn, S.; De Hosson, J.T.M.; Schulte, K.; Fiedler, B. Pressure and temperature induced electrical resistance change in nano-carbon/epoxy composites. *Compos. Sci. Technol.* 2015, 115, 1–8.

104. Novák, I.; Krupa, I. Electro-conductive resins filled with graphite for casting applications. *Eur. Polym. J.* 2004, 40, 1417–1422.
105. Moriche, R.; Sánchez, M.; Jiménez-Suárez, A.; Prolongo, S.G.; Ureña, A. Strain monitoring mechanisms of sensors based on the addition of graphene nanoplatelets into an epoxy matrix. *Compos. Sci. Technol.* 2016, 123, 65–70.
106. Wichmann, M.H.G.; Buschhorn, S.T.; Gehrman, J.; Schulte, K. Piezoresistive response of epoxy composites with carbon nanoparticles under tensile load. *Phys. Rev. B* 2009, 80, 245437.
107. Nanni, F.; Ruscito, G.; Puglia, D.; Terenzi, A.; Kenny, J.M.; Gusmano, G. Effect of carbon black nanoparticle intrinsic properties on the self-monitoring performance of glass fibre reinforced composite rods. *Compos. Sci. Technol.* 2011, 71, 1–8.
108. Nanni, F.; Auricchio, F.; Sarchi, F.; Forte, G.; Gusmano, G. Self-sensing CF-GFRP rods as mechanical reinforcement and sensors of concrete beams. *Smart Mater. Struct.* 2006, 15, 182–186.
109. Nanni, F.; Ruscito, G.; Forte, G.; Gusmano, G. Design, manufacture and testing of self-sensing carbon fibre–glass fibre reinforced polymer rods. *Smart Mater. Struct.* 2007, 16, 2368–2374.
110. Feller, J.F.; Linossier, I. Mechanical and rheological properties of poly(ethylene-co-ethyl acrylate) as a function of carbon black content. *Macromol. Symp.* 2003, 203, 317–324.
111. Droval, G.; Feller, J.F.; Salagnac, P.; Glouannec, P. Rheological properties of conductive polymer composite (CPC) filled with double percolated network of carbon nanoparticles and boron nitride powder. *e-Polymers* 2009, 9, 1–17.
112. Lagrève, C.; Feller, J.F.; Linossier, I.; Levesque, G. Poly(butylene terephthalate)/ poly(ethylene-co-alkyl acrylate)/ carbon black conductive composites: Influence of composition and morphology on electrical properties. *Polym. Eng. Sci.* 2001, 41, 1124–1132.
113. Pillin, I.; Feller, J.F. Influence of carbon-black nanoparticles on poly (butylene terephthalate) fractionated crystallization in bicomponent poly (butylene terephthalate)/poly (ethylene-co-ethyl acrylate) blends. *Macromol. Mater. Eng.* 2006, 291, 1375–1387.
114. Szeluga, U.; Kumanek, B.; Trzebicka, B. Synergy in hybrid polymer/nanocarbon composites: A review. *Compos. Part A Appl. Sci. Manuf.* 2015, 73, 204–231.

---

Retrieved from <https://encyclopedia.pub/entry/history/show/51515>